Pergamon

0306-4522(95)00344-4

Neuroscience Vol. 70, No. 1, pp. 191–200, 1996
Elsevier Science Ltd

0306-4522/96 $9.50 + 0.00

LOW DIMENSIONAL ATTRACTORS IN DISCHARGES OF SENSORY NEURONS OF THE RAT SPINAL DORSAL HORN ARE MAINTAINED BY SUPRASPINAL DESCENDING SYSTEMS

S. DEBUS and J. SANDKÜHLER*

II. Physiologisches Institut, Universität Heidelberg, Im Neuenheimer Feld 326, 69120 Heidelberg, Federal Republic of Germany

Abstract—Background activity was recorded from sensory neurons in laminae I–V of the lumbar spinal dorsal horn of the rat prior to and during cold block spinalization at the cervical cord. To graphically and quantitatively describe the complexity of the discharge patterns, phase space portraits were plotted and the correlation dimension D_2 was calculated by using the Grassberger–Procaccia algorithm adopted for point processes, i.e. for series of interspike intervals. The algorithm is validated both for the Baker transformation, which is a simple point process, and for the Lorenz model, whereby a transformation from continuous to point process variables is achieved. A method of surrogate data is provided in order to show the difference between original neuronal patterns and their surrogate stochastic data. Therefore, this method shows that neuronal discharge patterns cannot be fully described in terms of interspike interval histograms. However, in the intact cord most (73%) of the neurons displayed background activity with low (0.28–4.3) D_2 values.

During spinalization, D_2 values significantly increased in 68% of the neurons showing previously low D_2 values, irrespective of classification and laminar location of neurons, thus proving that tonic descending systems may maintain a high order in the discharge of sensory dorsal horn neurons.

Key words: discharge pattern, spinalization, nociception, correlation dimension, phase space, point process.

It is well known that sensory neurons in the spinal dorsal horn may display considerable background activity which is subjected to tonic descending modulation.[2,15] It is generally assumed that the action potentials are generated at random intervals, constituting a simple renewal process,[21] because some of the mechanisms underlying spike generation are apparently stochastic processes, as revealed by the open and closing times of ion channels[3] and peak amplitudes of unitary postsynaptic potentials.[22] The degrees of freedom in neuronal discharges may also be increased by up to 10^4 synapses converging on to one neuron. Previously employed counting statistics may, however, not securely discriminate stochastic from deterministic processes. Powerful analytical tools which are based on the ergodic theory[6] of non-linear dynamics have been established to describe non-linear dynamics either graphically, such as the phase space portrait,[23] or quantitatively, such as the correlation dimension D_2.[7]

The ergodic theory has shown that irregular patterns can be generated by functions with low degrees of freedom and that the dynamics are represented by an attractor with dimension D, which provides the number of degrees of freedom m and is, therefore, a parameter of the complexity of a system (e.g., white noise with $D = \infty$), periodic sequences as a discrete map of interspike intervals $D = 0$ (attractors with non-integer dimension are called "fractals"). There is also evidence that some neuronal systems exhibit chaotic attractors.[13] We have adopted these methods for the point process $P(t)$, which is constituted by the spike occurrence times of neuronal discharges.

EXPERIMENTAL PROCEDURES

Experimental design

Principle experimental procedures have been described in detail elsewhere.[16] Briefly, experiments were performed on male Sprague–Dawley rats under deep pentobarbital anesthesia. The trachea was cannulated to allow mechanical ventilation with room air. Pancuronium bromide (0.5 mg/kg) was given intravenously for muscle relaxation. One external jugular vein was cannulated for continuous infusion of a glucose tyrode solution, which also contained 15 mg/ml of sodium pentobarbital. The infusion rate was adjusted so that 30–60 mg/kg/perh of pentobarbital were given to maintain a deep level of anesthesia, which was verified by stable mean arterial blood pressure and a constant heart rate during noxious skin stimulation. One common carotid artery was cannulated to continuously monitor the mean arterial blood pressure, which ranged between 75 and 100 mmHg. Colorectal temperature was kept constant

*To whom correspondence should be addressed.

Abbreviations: GP, Grassberger–Procaccia; ISI, interspike interval; ISIH, interspike interval histogram.

at 37.5 ± 1°C (mean ± S.D.) by means of a feed-back controlled heating blanket underneath the ventral surface of the animal. The left sural nerve was dissected free for bipolar stimulation with platinum hook electrodes and left in continuity. The left hindpaw was fixed pad upwards with paraffin wax in a holder to allow noxious radiant heating of the glabrous skin. The lumbar enlargement and the upper cervical cord were exposed by laminectomy. All exposed nervous tissue was covered with warm paraffin oil.

Recording and stimulation

Extracellular recordings were made with tungsten microelectrodes (4–5 MΩ impedance at 1 kHz; A-M System, Inc.). Light mechanical probing at the left hindpaw was used as a search stimulus to identify neurons with a cutaneous mechanoreceptive field. The sizes of the receptive fields were determined by the use of a von Frey hair (6.7 g). Data collection was started no earlier than 20–40 min after a neuron was found.

The periods of continuous recording of the background activity were variable (5–30 min) to allow analysis of at least 650 action potentials; typically, 2000–5000 action potentials were recorded per neuron.

The sural nerve was stimulated electrically to recruit Aβ and Aδ fibers only (0.1 ms pulses, 2.5 V) or to excite both A and C fibers (0.5 ms pulses, 25 V). To identify neurons in lumbar cord with long ascending projections, cervical cord segments were electrically stimulated by bipolar surface electrodes attached bilaterally to the lateral funiculi. The antidromic response was characterized in the usual manner by a constant response latency and by following high-frequency stimulation (333 Hz). Noxious radiant skin heating consisted of 50°C stimuli given for 10 s in intervals not shorter than 2 min.

Neurons were classified according to their afferent input as class 1 (Aβ fiber input only, low-threshold cutaneous receptive field at the ipsilateral hindpaw), or as class 2 neurons (Aβ/Aδ and C fiber input, response to noxious radiant skin heating, 50°C, 10 s). Only neurons with considerable background activity (3.5–91 impulses/s) were used in this study. Recordings were digitized by an analog/digital converter card (DT2821) at 32 kHz and stored on an AT-compatible computer. Spike occurrence times were assessed with a time resolution of 0.1 ms.

Spinalization at the upper thoracic cord and decerebration

For reversible spinalization, a metal thermode (surface temperature 0–4°C) was placed directly on to the spinal cord dorsum at the seventh cervical to the second thoracic segments. In all animals, spinalization produced a fall in mean arterial blood pressure by 40–50%. In another series of experiments, animals were decerebrated by the four-vessel occlusion technique and surgical spinalization was made at the first cervical segment after local infiltration of lidocaine (2%). In these experiments, at least 4 h was allowed following the termination of pentobarbital before recording was begun.

Histology

At the end of each experiment an electrolytic lesion was made at the spinal recording site (30–40 μA, 20–25 s). The rats were killed with an overdose of pentobarbital and were transcardially perfused with phosphate-buffered saline followed by paraformaldehyde (4%). The spinal cord was removed and cut in a cryostat in 50-μm coronal sections. The sections were stained with Cresyl Violet and the recording site was identified.

The Grassberger–Procaccia algorithm

If the discharge pattern is modulated by tonic descending pathways, either by monosynaptic input or via a spinal neuronal network, then the point process $P(t)$ is a function of the descending modulation. Alternatively, the discharge pattern could remain unaffected. For the following the index "int" stands for background activity with cord "intact" and the index "spin" stands for the experimental condition, which is here the cold block "spinalization". From recordings we gain the point processes P_{int} and P_{spin}, but not their generating functions F_{int} and F_{spin}. Therefore, the neuronal activity P is usually analysed by mean discharge rates or by interspike interval histograms (ISIHs) or by estimating spectral density. However, these methods only allow a reduced "one-dimensional" view to the function F.

According to theory, it can be shown[6,22] that information regarding the degrees of freedom of the functions F_{int} and F_{spin} can also be achieved if only "one-dimensional" recordings (i.e. sampled data) are available. In our case, the general point process P is identified either by its occurrence time θ_i or by its interspike intervals (ISIs) $I_i = \theta_{i+1} - \theta_i$ or higher deviations, i.e. $I'_i = I_{i+1} - I_i$.

The procedure used here to estimate the dimension of the attractor is essentially that of Grassberger and Procaccia.[7] From a set of measured ISIs $\{I_i | i = 1, \ldots, N\}$ or their "deviations" $\{I'_i = | i = 1, \ldots, N\}$ a time delay vector $X_i = (I'_i, I'_{i+1}, \ldots, I'_{i+\tau*(m-1)})$ is formed in an m-dimensional embedding space. N is the number of intervals and τ is the time delay parameter. The movement of the vector in the embedding space builds up to the phase space portrait.

$$C_m(r) = \frac{1}{N^2} \sum_{\substack{i,j=1 \\ i \neq j}}^{N} H(r - |X_i^{(m)} - X_j^{(m)}|). \quad (1)$$

The time delay vectors are used [equation (1)] to calculate the correlation function $C_m(r)$. The Heavyside function H [$H(x) = 0$ if $x \leqslant 0$ and $H(x) = 1$ if $x > 0$] counts the vectors within scaling radius r.

$$D_2(m) = \lim_{\substack{r \to 0 \\ N \to \infty}} \frac{\mathrm{d} \log C_m(r)}{\mathrm{d} \log r}. \quad (2)$$

D_2 can be calculated from the slope of the logarithm of $C_m(r)$ [equation (2)], repeating the calculations for a series of increasing m (to $m = 2, \ldots, 20$) until a saturation plateau is found (Fig. 1). Plotting all values of $D_2(m)$ vs m, this function supplies the saturation curve (e.g. Fig. 5) and the asymptote gives an estimate of D_2. In the asymptotic region the slope of correlation function is independent of m. $C(r)$ is known to scale as $C(r) \sim r^{D_2}$. D_2 is called the correlation dimension. The intersection of saturation curve and asymptote yields the minimal embedding dimension m_{min}. m_{min} is a lower bound of the degree of freedom n (number of variables governing the underlying system F). If no plateau and no saturation is found for values of $D_2(m)$ larger than 10.0, then the correlation dimension has to be considered as "high". Beyond this limit the Grassberger–Procaccia (GP) algorithm becomes inaccurate.

The correlation function $C_m(r)$ supplies two different quantitative measures. (1) Non-integer values of D_2 suggest a fractal structure and possible (but not necessarily) chaotic dynamics. $D_2 \leqslant D$ is a lower bound to the Hausdorff dimension D. Low values of D_2 indicate that data are not purely stochastic if the GP algorithm is applied carefully. (2) The embedding dimension m_{min} defines a lower bound of embedding space, i.e. the number n of variables governing the process. The inequality $n \geqslant 2D_2 + 1$ holds, which gives a saturation condition.

Stationarity

We have excluded all non-stationary spike trains from further analysis. Stationarity is tested with average trend tests from ISIs, the phase frequency tests of Wallis and Moore and with the quick sign test of Cox and Stuart.[20,26]

Methods of surrogate data

Theiler[25] has suggested a method of surrogate data for time series which is in short: (i) fourier transformation of data; (ii) randomizing the phase coefficients; (iii) back

transformation. The aim of this method is to produce a set of new "surrogate" time series with the same statistical properties (spectrum, mean, variance) but with a loss of correlation in phase space. Here, we produce surrogates of point processes by randomizing ISIs (Fig. 3). If the results of the computation D_2 on the surrogates are significantly different from the original, then it can be shown that the original is not just linearly correlated noise.[25]

Methods of validation

Because we reconstruct the phase space of a neuronal dynamic system with the point process variable I', it is necessary to examine whether or not this variable preserves the information of the original dynamic system. We have validated the GP algorithm for the variable I' with a known theoretical point process. Here, we use the Baker transformation,[18] which is defined through the equation:

$$x_{n+1} = 2x_n \bmod 1$$

$$y_{n+1} = \begin{cases} Ay_n & \text{for } 0 \leqslant x_n < \frac{1}{2} \\ \frac{1}{2} + Ay_n & \text{for } \frac{1}{2} \leqslant x_n \leqslant 1. \end{cases} \quad (3)$$

The variable y corresponds to our interspike variable I. I' is gained by difference building. Using more variables y, the Baker transformation can be generalized to more than one dimension, with known theoretical Hausdorff dimension D. Hence, we are able to decide whether information about the reconstructed attractor is preserved in the variable I' and to determine the accuracy of the GP algorithm on evaluating the correlation dimension D_2.

One important question may arise: which point process variable, I or I', contains the decisive information about the dynamic system? To find an answer, we have reconstructed the phase space of the most frequently examined standard Lorenz model (Z_1, Z_2, Z_3 with $s = 10.0$, $r = 28.0$, $b = 8/3$) in our point process variables I and I', and we have compared the results of D_2 with the known theoretical values of the Lorenz attractor:

$$\dot{Z}_1 = -sZ_1 + sZ_2$$

$$\dot{Z}_2 = -Z_1Z_3 + rZ_1 - Z_2$$

$$\dot{Z}_3 = Z_1Z_2 - bZ_3. \quad (4)$$

The change from continuous variables to point process variables has been performed by the following transformation. Following Lorenz,[11] we have evaluated the maximum M_i ($i = 1, \ldots, N$) of each variable Z_k (k 1, 2, 3). In order to simplify matters, we confine to variable Z_3 and omit index 3. Plotting two consecutive maxima of Z (M_i vs M_{i+1}), this yields the usual discretized first return map of the Lorenz model, which may be interpreted as its Poincaré section. To prove the validity of our point process variables I and I', we have registered the "occurrence time" θ of the maximum of Z, i.e. we have discretized the continuous Lorenz variable Z to a point process with the discrete "event" variable θ. In general, all information which is contained in M_i ($i = 1, \ldots, N$) should be preserved in the occurrence time variables θ_i (according to all Z_k, M_k, θ_k, $k = 1, 2, 3$). From the θ_i variables we gain the appropriate variables I_i and I_i', and at this time we are able to decide whether I_i or I_i' is more suitable to reconstruct the known properties of the Lorenz model.

RESULTS

The Baker transformation

The point process variable I', generated by the Baker transformation, was analysed with the GP algorithm. The correlation dimension D_2 was compared with the theoretically known Hausdorff dimension D. The results are given in Table 1.

The statistical errors are standard deviations of the slope estimated by least square fits. Our findings are in good agreement with the known theoretical

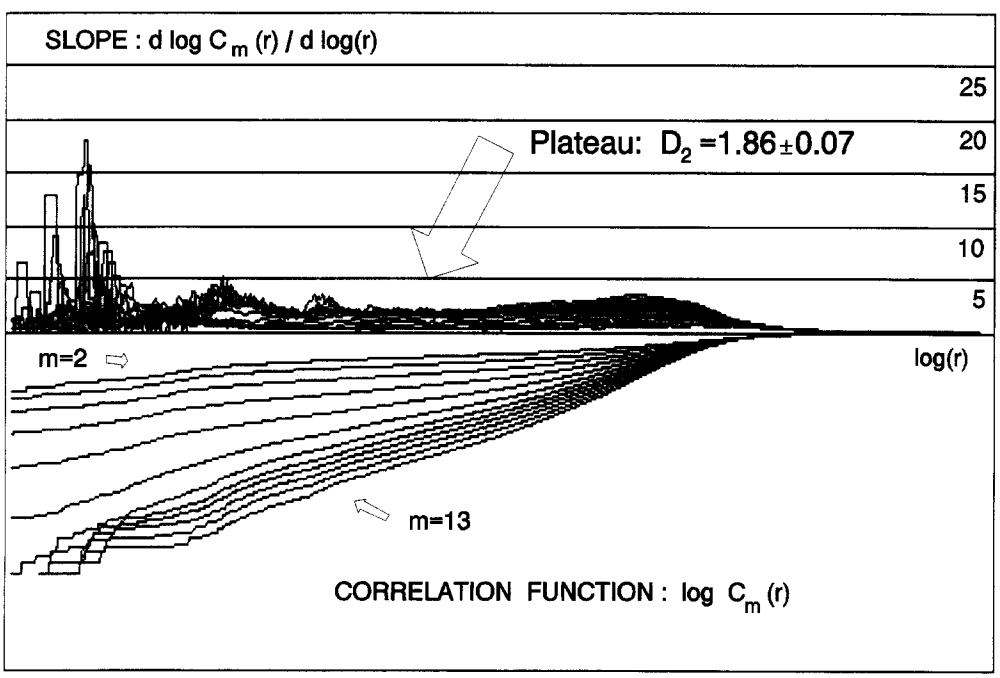

Fig. 1. Correlation function ($D_2 = 1.86$) of background activity of a neuron recorded with cord intact (neuron 25 in Table 2, class 2, lamina IV) is shown in the lower part and the logarithm of its first deviation in the upper part of the figure. The wide plateau indicates good scaling properties.

Table 1. Validation of the Grassberger–Procaccia algorithm for a point process (the Baker transformation) and its generalization to more than two variables (see Schuster[18]) with theoretical Hausdorff dimension D

The Baker transformation with various constants	GP algorithm: correlation dimension D_2	The Hausdorff dimension D of the Baker transformation
$A = 0.22639$	0.512 ± 0.291	0.466
$A = 0.37316$	0.725 ± 0.095	0.703
$A = 0.44817$	0.884 ± 0.038	0.864
$A = 0.48922$	0.977 ± 0.024	0.968
$A = 0.44817$ (two variables)	1.815 ± 0.059	1.864
$A_1 = 0.44817$ $A_2 = 0.37316$ (four variables)	3.431 ± 0.407	3.567

Hausdorff dimension D. Theoretical values lie within margins of error (Table 1).

The Lorenz model

Constructing the phase space of the Lorenz model with the point process variables, we have found that the variable I'_3 (derived from Z_3) and the first return map (M_i vs M_{i+1}) of the original variable Z_3 have the same phase space portrait[11,19] (Fig. 2). Relevantly, this does not hold for variable I_3. Estimating D_2 and using the appropriate variable I', we have found $D_2 = 1.04 \pm 0.06$ (on I'_1 derived from variable Z_1), $D_2 = 1.09 \pm 0.06$ (on I'_2 derived from variable Z_2) and $D_2 = 1.16 \pm 0.21$ (on I'_3 derived from variable Z_3). These results are in good agreement with the theoretical dimension $D = 1.06$ on the Poincaré section.[19]

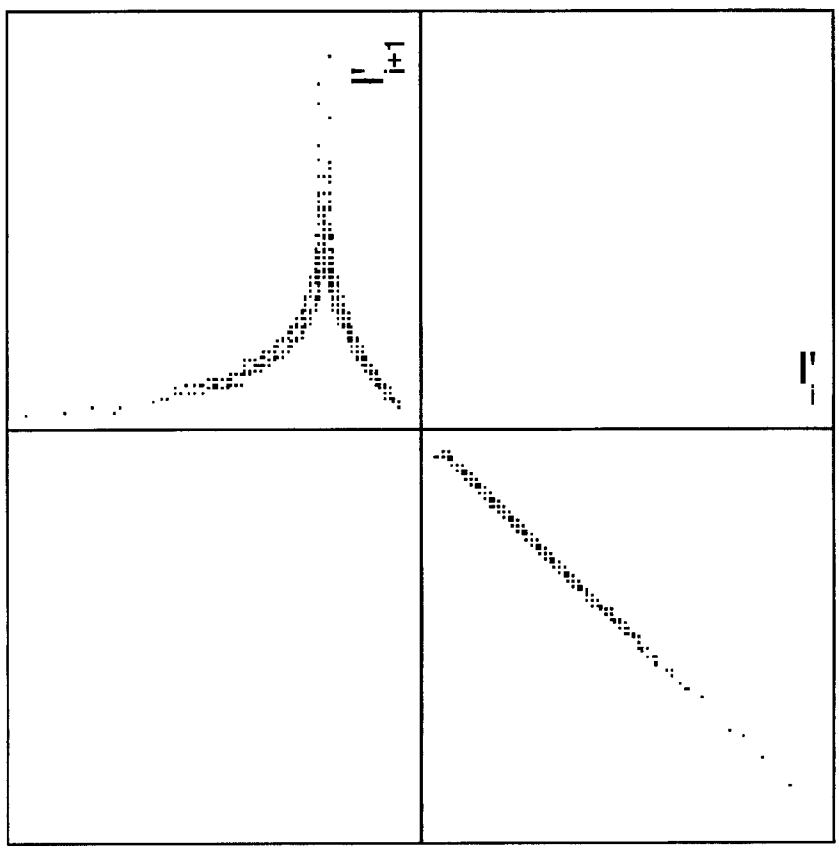

Fig. 2. Unusual phase space portrait of the Lorenz model in time delay coordinates of variable I' (coordinates in arbitrary time units). With the exception of the straight line in the lower right quadrant, which is simply a product of projection from three to two embedding dimensions, the portrait is identical to the first return map[11,18] of the usual variable Z_3 [see notation of variables in equation (4)]. Importantly, only the variable I', and not I, is able to reconstruct the usual Poincaré section.

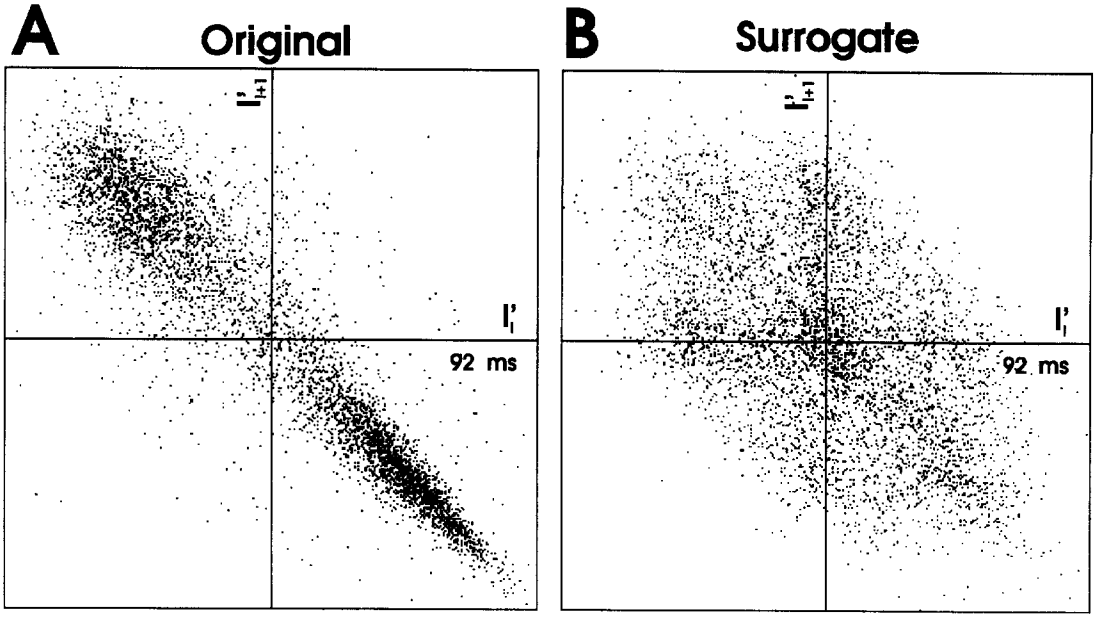

Fig. 3. Phase space portrait of original neuronal discharge (A; neuron 24 in Table 2) and its surrogate (B). The correlation dimension increases (from $D_2 = 0.96$ to $D_2 =$ high) by randomizing intervals.

Surrogate

Figure 3 shows the phase space of the original background discharge (A) of a neuron and its surrogate (B). Figure 4 shows the ISIH which is, of course, identical for both the original and surrogate with the same mean and variance. Figure 5 shows the different saturation behavior: the original with good saturation properties ($D_2 = 0.96 \pm 0.03$) and the surrogate with no saturation ($D_2 =$ high) within the range of embedding dimension $m = 2$–20. The randomized surrogate data do not show the same behavior in the saturation diagram as in white noise. This can be explained by the weak structure of the surrogate in the phase space (Fig. 3B) (see Discussion).

Spinalization

Results were obtained from a total of 26 neurons recorded in laminae I–V of the lumbar spinal dorsal horn. Four neurons were low-threshold (class 1) neurons; the remaining 22 neurons were multireceptive (class 2) neurons.

With the spinal cord intact, 19 (73%) of the

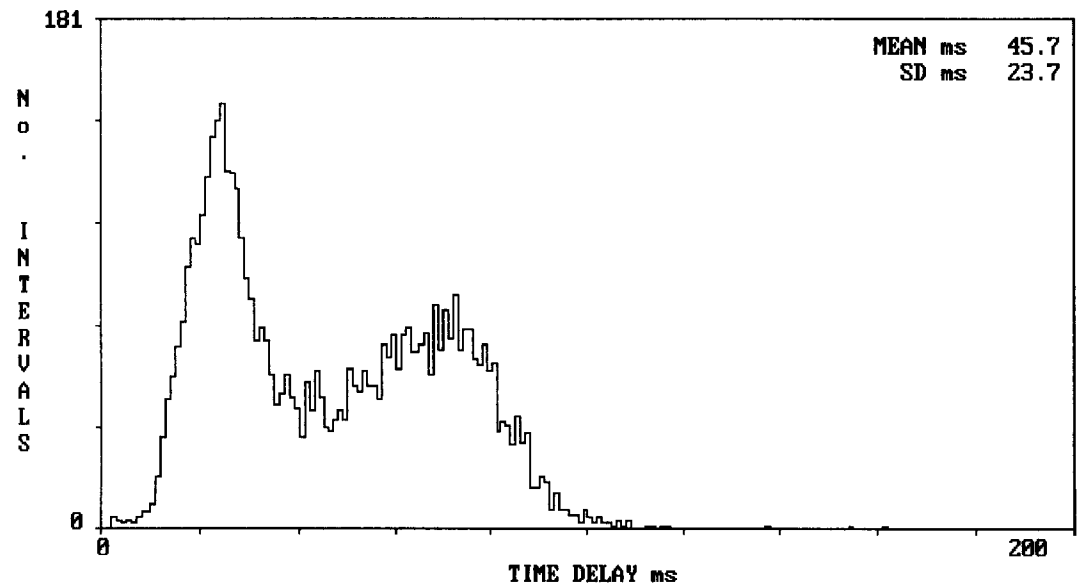

Fig. 4. Identical ISIH of the original neuronal discharge and its surrogate (neuron 24). The identity of the histograms and of statistical descriptions such as mean and S.D. shows that complex patterns cannot be fully described in terms of the ISIH.

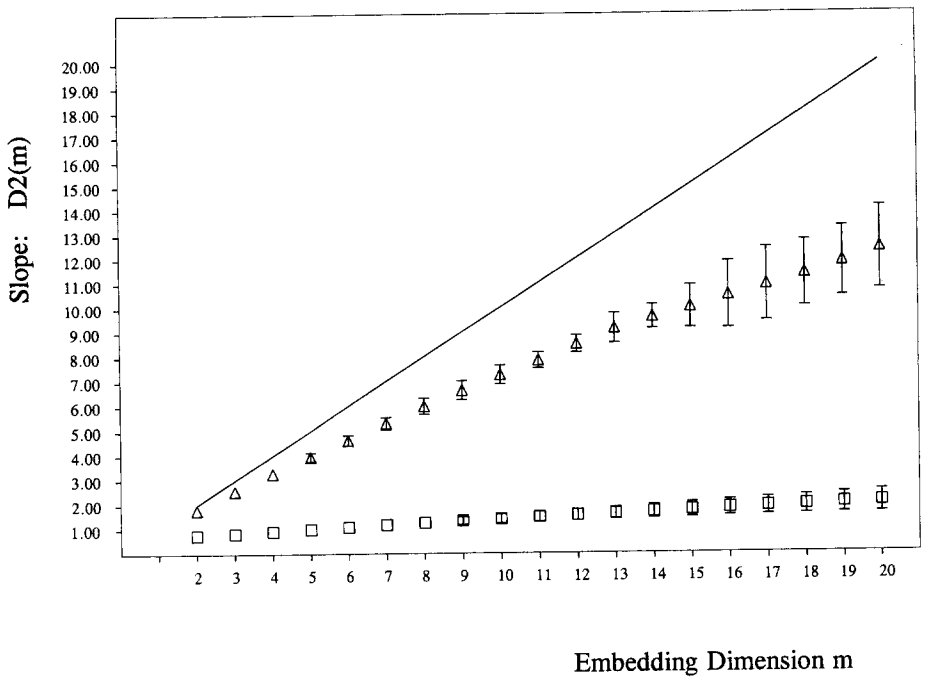

Fig. 5. Saturation diagram: slope of $\log C_m(t)$ vs embedding dimension m of original (□) and surrogate (△) data (neuron 24). The figure shows low $D_2 = 0.96 \pm 0.03$ for the neuronal pattern and no saturation (D_2 = high) for the randomized surrogate data. The solid line symbolizes theoretical white noise.

neurons displayed background activity with D_2 values below 5 and three of the neurons had a second plateau in the correlation function, all of which also revealed D_2 values below 5. Phase space portraits revealed characteristic patterns (see Fig. 6 for examples). Seven neurons had "high" D_2 values larger than 10 before and after spinalization.

After spinalization, D_2 values significantly increased in 13 of 19 neurons (68%) with previously low D_2 values [in one neuron (No. 11 in Table 2), a second plateau revealed an unchanged D_2 value; two of the neurons were class 1 neurons]. D_2 values remained unchanged in three of 19 neurons (16%); in one neuron (No. 11) a second plateau revealed an increased D_2 value and in two neurons only very small but significant decreases (ΔD_2: -0.6 and -0.9, respectively) were evident. The D_2 values of all seven neurons with "high" D_2 values with the cord intact remained "high" during spinalization; thus, no change in the D_2 values could be determined.

The increases in the D_2 values during spinalization were detected irrespective of the classification and laminar location of the neurons (see Table 2). However, in all five neurons which displayed increased mean ISIs during spinalization (Nos 6, 11, 19, 22 and 25), the D_2 values also increased significantly.

DISCUSSION

From a methodological and physiological point of view, it is not conclusive to apply a stochastic analysis, such as averaging, to determine mean discharge rates to non-stochastical variables, as it would be impossible to define a "true" mean value characterizing a single "true" state of the system. A deterministic system may rather be characterized by multiple or by no stable states. Furthermore, averaging of neuronal discharge rates is often applied for bin widths of one or more seconds, i.e. for time intervals far beyond the duration of postsynaptic potentials. Thus, mean discharge rates may not always provide biologically meaningful parameters of non-stochastical neuronal activity.

Choice of variables

We have therefore developed a phase space portrait for point processes and quantitatively determined the complexity of the spike train. Any possible variable which represents the properties of a dynamic system may be used to determine the dimension of the underlying attractor. For the following reasons we suggest that the variable I' is the most suitable. (1) We know from our numerical studies on the standard Lorenz model with variables Z_1, Z_2 and Z_3 that the variable I' (derived from Z_3) and not the interval variable I represents the dynamic structure (the Poincaré section) of the Lorenz attractor. Upon availability of the point process variable θ, we maintain that I' is more suitable than I in representing the dynamic behavior. (2) Schechtman *et al.*[18] found that the variable I' removes the dominant characteristic apparent in the phase space portrait, i.e. a possible strong positive correlation between one interval and

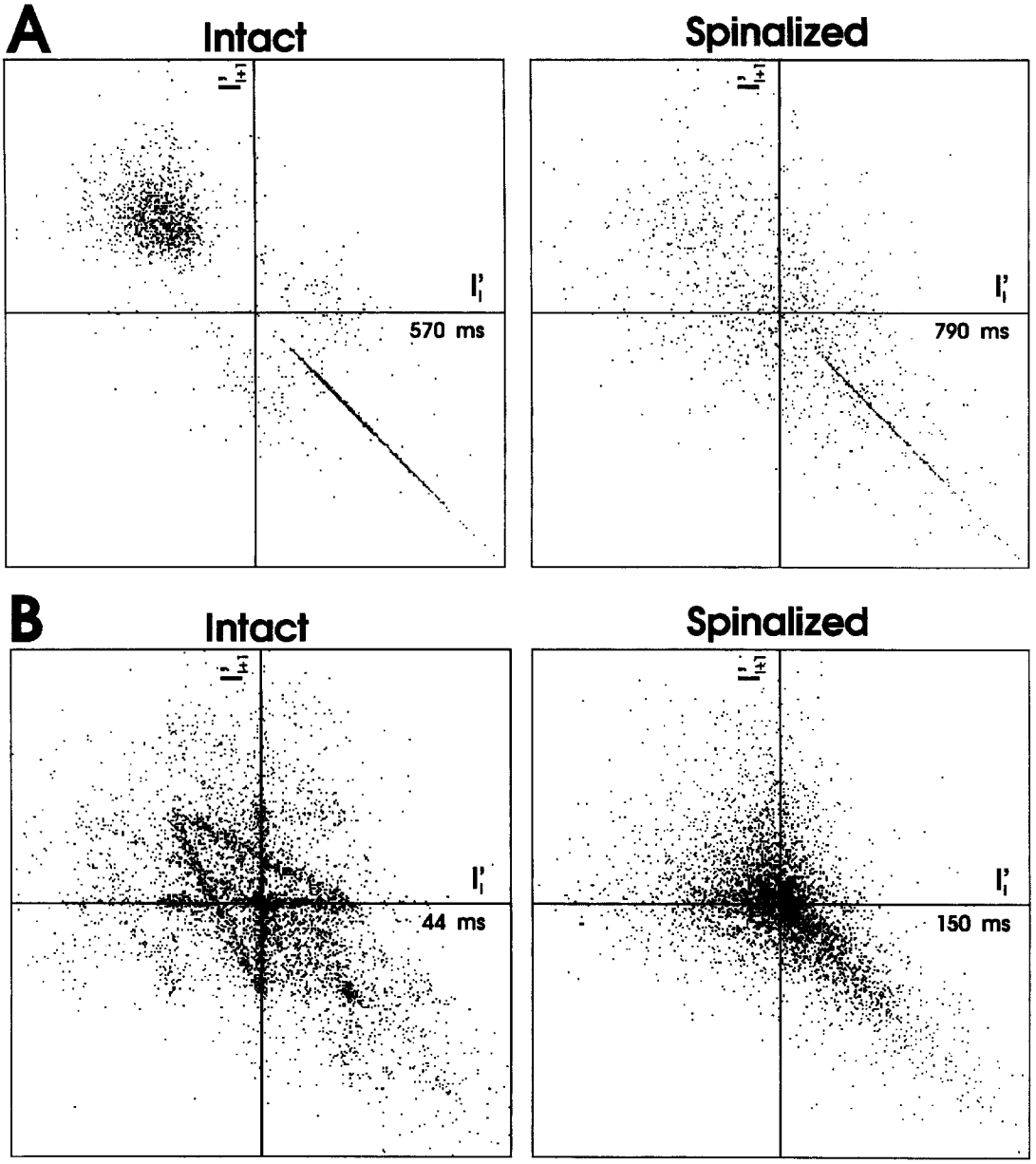

Fig. 6. Discharge activity of two neurons [one neuron of an older data set (A) and neuron 19 in Table 2 (B)] in phase space portrait. Loss of order during cold block spinalization ("Spinalized") is seen clearly (right-hand phase portraits) as compared to the more ordered background activity with cord intact ("Intact"; left).

the next. (3) The variable I' has zero average, which entails simplification in statistical calculations, e.g. moments and cumulants of statistical models. (4) All intervals I_i are positive, but values of I' range from minus to plus. Consequently, the phase space is not restricted to the positive quadrant in two up to m embedding dimensions. (5) It is generally advantageous to gain a broad scaling region[24] in the correlation function. Because of the logarithmic behavior of the GP algorithm, a simple positive scaling of the interval variable I will not produce a "broadening", but only a shift of the correlation function to higher values of r. However, the variable I' shows the desired "broadening" effect.

Problems of stationarity of the dynamic process

We tested the stationarity of neural discharge rates and excluded all "non-stationary" spike trains. However, these tests are only of limited use. For example, mean discharge rates could be changed simply by scaling all ISIs with some fixed factors. In any case, the complexity of the system would not change, because the correlative relation of data points in the phase space remains undisturbed by scaling. This means, however, that the phase space is invariant under the scaling operation, as can be seen in "spreading" or "shrinking", which does not change the statistical properties of $C(r)$. On the other

Table 2. Summary of results

Neuron			Cord intact ("int")			Spinalization ("spin")			Changes: int → spin	
1	2	3	4	5	6	7	8	9	10	11
No.	Class	Lamina	Mean I	N	D_2	Mean I	N	D_2	Mean	D_2
1	1	V	0.1275	3800	2.13 ± 0.10	0.0469	3800	2.92 ± 0.37	−−	++
2	1	III	0.0244	8900	1.08 ± 0.10	0.0144	8900	1.17 ± 0.06	−	+
3	2	III	0.0615	4200	1.63 ± 0.07	0.0515	4200	High	−	++
4	1	IV	0.0203	8500	3.00 ± 0.32	0.0119	8500	High	−−	++
5	2	I	0.0448	4400	0.60 ± 0.06	0.0314	4400	0.84 ± 0.02	−−	++
6	2	I	0.0296	4800	4.30 ± 0.81	0.0405	4800	High	++	++
7*	2	I	0.2170	650	0.56 ± 0.06	0.1824	650	0.45 ± 0.12	−−	−
8*	2	V	0.1480	750	High	0.0222	8500	High	−−	n.d.
9*	2	V	0.1860	640	1.60 ± 0.41	0.0515	5400	High	−−	++
10	1	V	0.1163	1080	High	0.0419	6200	High	−−	n.d.
11A	2	III	0.0139	5100	0.64 ± 0.02	0.0152	5100	0.66 ± 0.01	+	+
B					3.81 ± 0.09			High	+	++
12	2	III	0.0110	8100	3.19 ± 0.34	0.0101	8100	High	−−	++
13	2	III	0.0120	7400	0.52 ± 0.02	0.0101	7400	0.46 ± 0.03	−−	−−
14	2	III	0.0292	3100	0.28 ± 0.03	0.0237	3100	0.19 ± 0.02	−−	++
15	2	III	0.0142	6200	High	0.0135	6200	High	−	n.d.
16	2	I	0.1883	1040	High	0.0665	1040	High	−−	n.d.
17	2	V	0.0387	5100	0.75 ± 0.09	0.0189	5100	2.88 ± 0.10	−−	++
18A	2	IV	0.2855	340	0.96 ± 0.04	0.0767	7800	High	−−	++
B*					1.04 ± 0.13			High	−−	++
19	2	IV	0.0148	4400	1.87 ± 0.04	0.0291	4400	High	++	++
20*	2	I	0.1890	750	0.46 ± 0.05	0.0429	7400	1.01 ± 0.06	−−	++
21	2	II	0.0564	2600	High	0.0220	2600	High	−−	n.d.
22A	2	IV	0.0243	3700	0.90 ± 0.02	0.0265	3700	1.00 ± 0.03	+	++
B					1.75 ± 0.23			2.83 ± 0.18	+	++
23	2	V	0.0501	2000	High	0.0461	2000	High	−	n.d.
24	2	V	0.0458	2100	0.87 ± 0.02	0.0457	2100	0.96 ± 0.03	−	++
25	2	IV	0.0417	2300	1.86 ± 0.07	0.0444	2300	1.96 ± 0.11	++	+
26	2	IV	0.0766	1300	High	0.0738	1300	High	−−	n.d.

Column 1: index of neuron; column 2: class of neuron (1, low threshold; 2, multireceptive); column 3: laminae I–V referred to Rexed;[14] columns 4 and 7: mean values of ISIs; columns 5 and 8: number N of analysed ISIs; columns 6 and 9: correlation dimension D_2; columns 10 and 11: changes in mean values and D_2 from background activity (int) to spinalization condition (spin); column 10: +, −, non-significant changes; ++, −−, significant changes (the Mann–Whitney test) of mean ISI values; column 11: +, −, tendency within statistical error and ++, −−, changes beyond statistical error of correlation dimension D_2 (n.d., no change determined). In three cases (Nos 11, 18 and 22) we found two attractors on different scales of the correlation function in the same process, each designated by the letters A and B. Thus, 29 scaling plateaux were present and analysed in 26 neurons.

hand, it is possible to find changes in the correlative relations between intervals without any changes in mean discharge rates. Consequently, statistical stationarity yields only a first indication of dynamic stability, but no sure indication of stability of neuronal time patterns.

The correlation dimension D_2

The quantitative determination of the D_2 correlation dimension allows estimation of the minimal number of degrees of freedom which underlie the dynamic process. Some caveats have to be taken into account when interpreting D_2, because there are several sources of possible artifacts which could lead to under- or overestimation[1,4,5,24] of D_2 and differentiate in point processes and time series. In the latter, D_2 depends on an equidistant sampling rate f_s. Oversampling could introduce too much correlation between data points and could cause an underestimation of D_2. Blind application of the GP algorithm could lead to low values of D_2 if sampling frequency is too high compared with the dominant periods of the system. In point processes, this kind of artifact does not exist, because oversampling would only increase the accuracy of the occurrence times θ of the spike train. Only undersampling would cause a loss of accuracy of occurrence time, and this would introduce system noise and overestimation of D_2. Here, undersampling is unlikely due to a time resolution of 0.1 ms.

Furthermore, in time series we have a defined relation between episode length T and the number of samples, $N = f_s T$, which does not hold in point processes. From our own studies with electroencephalogram time series,[4] we know that stable results can be achieved if T is at least 24 s. With an electroencephalogram sampling rate of 85 Hz, we analysed at least $N = 2000$ data points. Our experience with point processes (Debus and Sandkühler, unpublished observations) shows the same tendency: stable results of D_2 require at least $N = 2000$ samples. Smaller samples (i.e. $N = 1000$) are acceptable if one could test stationarity of D_2, for example, with descending N (here $N = 1000$–7000). Small differences referring

to samples with $N < 1000$ should not be overinterpreted because they may yield estimators of D_2 with relatively low precision (see neurons 7, 8, 9, 18 and 20, which are marked with an asterisk).

Surrogate data

The method of surrogates has shown that ISIHs do not reflect the whole complexity of point processes, because surrogates have the same mean, variance and ISIH as the original spike train, but the patterns and correlation dimension D_2 in phase space are completely different. Thus, the dynamic behavior of the discharge cannot be described in terms of ISIHs.

We have sometimes recognized typical patterns in phase space which appeared in the original point process and also in the surrogates. So, we can conclude that these patterns are only generated through the limited variability of ISIs and not through a dynamic system. Since D_2 detects correlations in the phase space of any kind (including linearly correlated noise), we should be careful not to misinterpret low values of D_2: if the original and the surrogate do not differ, then low D_2 values do not reflect the attractor dimension of a simple deterministic process. On the other hand, if the surrogate shows random patterns with high dimension, which can be distinguished from an ordered pattern of the original spike train (Fig. 2), then we conclude that D_2 is an indicator of a low dimensional deterministic process.

Background activity of spinal dorsal horn neurons

The present study has shown that background activity of many of the sensory neurons recorded in the spinal dorsal horn is not stochastic "noise", but results from deterministic processes with a low number of degrees of freedom, apparently overruling the spike generating mechanisms which have potentially infinite degrees of freedom. Since recordings were made under pentobarbital anesthesia, it cannot be excluded that the low D_2 correlation dimension was affected by suppressing the activity of afferent neurons. However, spinalization, which strongly reduces the number of afferents to a spinal neuron, did not decrease but increased the D_2 correlation dimension. Thus, the complexity of the discharge pattern is not simply a function of the number of active neurons converging onto the neuron under study. Furthermore, in another series of experiments, recordings were made in unanesthetized, decerebrate, spinalized animals. The D_2 correlation dimension of background activity of five class 2 and two class 1 neurons was similar to the values obtained in spinalized animals under pentobarbital anesthesia (data not shown). In these experiments, at least 4 h was allowed following the termination of pentobarbital infusion before recordings were begun.

The putative role of some of the discharge patterns is readily apparent: trains of clustered action potentials (bursts) should favor temporal summation, e.g. at the postsynaptic membrane and probably also the release of large dense-cored vesicles,[8,9] while harmonic oscillation (of sensory thalamic relay neurons) may indicate the presence of a transfer block for information[12] and may favor the second messenger-mediated effects.[10] One can only speculate about the role of more complex discharge patterns: if in reverberant pathways the conduction time corresponds to the duration of interburst intervals, then the effects of a feedback loop will be greatly enhanced. Furthermore, the duration of bursts and the intraburst discharge frequency may determine whether or not thresholds in the postsynaptic neurons are reached.

Descending modulation of spinal neuronal discharge patterns

Descending modulation of discharge patterns of spinal dorsal horn neurons remains undetected if only mean discharge rates are assessed Intuitively, one may expect that removal of any input to a neuron (e.g. by spinalization) should reduce the degree of freedom of its discharges. However, our results have shown that, in the majority of spinal dorsal horn neurons, D_2 values significantly increase during spinalization, irrespective of classification or laminar location of the neuron.

Descending modulation could be understandable as a reduction of states of the neurons, which behave as "slaves" under the rule of supraspinal systems. Thus, it appears to be a general principle that tonic descending systems may maintain high order in the discharges of sensory dorsal horn neurons. This could be a prerequisite for proper spinal cord function. If so, the spinal shock syndrome, seen in many species after acute spinal cord transection, could be a result of a loss of order in spinal neuron function.

The three neurons which displayed no significant change in the correlation dimension of their background activity could have rather simple intrinsic dynamics which are expressed independently of the supraspinal systems, as can be found in pacemaker neurons. Alternatively, these neurons could be integrated in a local neuronal network which, independently of the brain, generates simple dynamics.

In three of the neurons, two plateaux were identified in the correlation function; in two of these neurons spinalization selectively affected the pattern of long ISIs (10–50 ms time scale in neurons 11B and 22B), whereas the dimensionality of the discharges on the short time scale (2–5 ms) remained unaffected. Possibly, in these neurons the timing of long vs short ISIs could be caused by independent mechanisms (e.g., intrinsic cellular vs local network), which may be affected differentially by the supraspinal descending system.

In conclusion, our work has shown for the first time that background activity of many sensory neurons in the spinal dorsal horn is not stochastic, but results from deterministic processes with a low

number of degrees of freedom. This high order in discharge pattern is maintained in part by supraspinal descending modulation.

SUMMARY AND CONCLUSIONS

(1) Background activity was recorded from sensory neurons in laminae I–V of the lumbar spinal dorsal horn before and during cold block spinalization at the cervical cord.

(2) To graphically and quantitatively describe the complexity of the discharge patterns, we have plotted phase space portraits and calculated the correlation dimension D_2 with the GP algorithm, which we have adopted for point processes, i.e. for series of ISIs. A method of surrogate data was used to show the difference between original neuronal patterns and their surrogate noisy data.

(3) With the cord intact, most (73%) of the neurons displayed background activity with low (0.28–4.3) D_2 values. During spinalization, D_2 values significantly increased in 68% of the neurons with previously low D_2 values, irrespective of the classification and laminar location of the neuron.

(4) Thus, tonic descending systems may maintain high order in discharges of sensory dorsal horn neurons; this may be a prerequisite for proper spinal cord functions.

REFERENCES

1. Babloyantz A. (1990) Estimation of correlation dimension from single- and multichannel recordings—a critical view. In *Springer Series in Brain Dynamics* (ed. Babloyantz A.), pp. 123–130. Springer, Berlin.
2. Besson J. M. and Chaouch A. (1987) Peripheral and spinal mechanisms of nociception. *Physiol. Rev.* **67,** 67–186.
3. Colquhoun D. and Hawkes A. G. (1981) On the stochastic properties of single ion channels. *Proc. R. Soc. Lond.* **B211,** 205–235.
4. Debus S. (1992) Emotion und Chaos im Elektroenzephalogramm. Thesis, Medicine School Hannover, Hannover.
5. Debus S. and Künkel H. (1990) Chaotic dynamics of EEG in long-term studies. *Clin. Neurophysiol.* **20,** 62.
6. Eckman J. P. and Ruelle D. (1985) Ergodic theory of chaos and strange attractors. *Rev. mod. Phys.* **57,** 617–638.
7. Grassberger P. and Procaccia I. (1983) Measuring the strangeness of strange attractors. *Physica* **9D,** 189–208.
8. Harris-Warrick R. M. and Marder E. (1991) Modulation of neural networks for behavior. *A. Rev. Neurosci.* **14,** 39–57.
9. Iverfeldt K., Serfözö P., Diaz-Arnesto L. and Bartfai T. (1989) Differential release of coexisting neurotransmitters; frequency dependence of the efflux of substance P, thyrotropin releasing hormone and [^{3}H] serotonin from tissue slices of rat ventral spinal cord. *Acta physiol. scand.* **137,** 63–71.
10. Li Y.-X. and Goldbeter A. (1992) Pulsatile signaling in intracellular communication. Periodic stimuli are more efficient than random or chaotic signals in a model based on receptor desensitization. *Biophys. J.* **61,** 161–171.
11. Lorenz E. N. (1963) Deterministic nonperiodic flow. *J. atmos. Sci.* **20,** 130–141.
12. McCormick D. A. and Feeser H. R. (1990) Functional implications of burst firing and single spike activity in lateral geniculate relay neurons. *Neuroscience* **39,** 103–113.
13. Rapp P. E., Zimmermann I., Albano A. and DeGuzman G. (1985) Dynamics of spontaneous neural activity in the simian motor cortex. *Phys. Lett.* **A110,** 335–338.
14. Rexed B. (1952) The cytoarchitectonic organization of the spinal cord in the cat. *J. comp. Neurol.* **96,** 415–495.
15. Sandkühler J., Fu Q.-G. and Zimmermann M. (1987) Spinal pathways mediating tonic or stimulation-produced descending inhibition from the periaqueductal gray or nucleus raphe magnus are separate in the cat. *J. Neurophysiol., Bethesda* **58,** 327–341.
16. Sandkühler J., Willmann E. and Fu Q.-G. (1991) Characteristics of midbrain control of spinal nociceptive neurons and nonsomatoşensory parameters in the pentobarbital-anesthetized rat. *J. Neurophysiol., Bethesda* **65,** 33–48.
18. Schechtman V. L., Raetz S. L., Harper R. K., Garfinkel A., Wilson A. J., Southall D. P. and Harper R. M. (1992) Dynamic analysis of cardiac *R–R* intervals in normal infants and in infants who subsequently succumbed to the sudden infant death syndrome. *Pediatr. Res.* **31,** 606–612.
19. Schuster H. G. (1988) *Deterministic Chaos.* VCH Verlagsgesellschaft, Weinheim.
20. Soto E., Echagüe J. V. and Vega R. (1989) Computer program for statistical Mann–Whitney *U* non-parametric analysis of neuronal activity. *Comput. Meth. Program. Biomed.* **28,** 197–200.
21. Steedman W. M. and Zachary S. (1990) Characteristics of background and evoked discharges of multireceptive neurons in lumbar spinal cord of cat. *J. Neurophysiol., Bethesda* **63,** 1–15.
22. Stern P., Edwards F. A. and Sakmann B. (1992) Fast and slow components of unitary EPSCs on stellate cells elicited by focal stimulation in slices of rat visual cortex. *J. Physiol., Lond.* **449,** 247–278.
23. Takens F., Braaksma B. L. J. and Broer H. W. (1985) On the numerical determination of the dimension of an attractor. In *Lecture Notes in Mathematics* (ed. Braaksma B. L. J.), p. 99. Springer, Berlin.
24. Theiler J. (1986) Spurious dimension from correlation algorithm applied to limited time series data. *Phys. Rev.* **A34,** 2426–2432.
25. Theiler J. (1991) Some comments on the correlation dimension of $1/f^{\alpha}$ noise. *Phys. Lett.* **A155,** 480–493.
26. Wang D. C. C. and Vagnucci H. (1980) Tsan: a package for time series analysis. *Comput. Programs Biomed.* **11,** 132–144.

(*Accepted* 7 *August* 1995)